Research Article

Porous Silica-Supported Solid Lipid Particles for Enhanced Solubilization of Poorly Soluble Drugs

Rokhsana Yasmin,[1] Shasha Rao,[1] Kristen E. Bremmell,[1] and Clive A. Prestidge[1,2]

ABSTRACT. Low dissolution of drugs in the intestinal fluid can limit their effectiveness in oral therapies. Here, a novel porous silica-supported solid lipid system was developed to optimize the oral delivery of drugs with limited aqueous solubility. Using lovastatin (LOV) as the model poorly water-soluble drug, two porous silica-supported solid lipid systems (SSL-A and SSL-S) were fabricated from solid lipid (glyceryl monostearate, GMS) and nanoporous silica particles Aerosil 380 (silica-A) and Syloid 244FP (silica-S) *via* immersion/solvent evaporation. SSL particles demonstrated significantly higher rate and extent of lipolysis in comparison with the pure solid lipid, depending on the lipid loading levels and the morphology. The highest lipid digestion was observed when silica-S was loaded with 34% (*w/w*) solid lipid, and differential scanning calorimeter (DSC) analysis confirmed the encapsulation of up to 2% (*w/w*) non-crystalline LOV in this optimal SSL-S formulation. Drug dissolution under non-digesting intestinal conditions revealed a three- to sixfold increase in dissolution efficiencies when compared to the unformulated drug and a LOV-lipid suspension. Furthermore, the SSL-S provided superior drug solubilization under simulated intestinal digesting condition in comparison with the drug-lipid suspension and drug-loaded silica. Therefore, solid lipid and nanoporous silica provides a synergistic effect on optimizing the solubilization of poorly water-soluble compound and the solid lipid-based porous carrier system provides a promising delivery approach to overcome the oral delivery challenges of poorly water-soluble drugs.

KEY WORDS: formulation; oral delivery; poorly soluble drugs; porous silica; solid lipid.

INTRODUCTION

Poor aqueous solubility and limited dissolution in the gastrointestinal tract (GIT) are known to be the major cause of low and variable oral bioavailability for Biopharmaceutical Classification System (BCS) class II drugs (1–4). For example, lovastatin (LOV), an anti-hypercholesterolemic agent, exhibits low aqueous solubility (0.4 μg/ml), extensive first-pass metabolism, short half-life, significant effect of food intake on oral drug absorption, and hence less than 5% oral bioavailability (5,6). Lipid-based drug delivery systems (LBDDS) including emulsion (micro/nano) (7,8), liposomes (9), self-emulsifying systems (SEDDS/SNEDDS) (10), solid lipid nanoparticles (SLN) (11,12), and nanostructured lipid carriers (NLC) (6,13) have been formulated to overcome these hurdles and therefore improve the oral bioavailability of

LOV. For instance, incorporating LOV into a NLC dispersion has led to three- to sixfold improvement in oral bioavailability compared to the unformulated drug in a rat model.

On the other hand, mesoporous silica nanoparticles have attracted enormous attention in recent years as an efficient drug carrier for poorly soluble drugs. Porous silica has excellent physicochemical properties such as small pore size, high surface area condensed with silanol groups, and high pore volume. This provides benefits in high drug loading capacity and preserves the encapsulated drug in an amorphous state which exhibits higher solubility (14–16). A recent study suggested that the altered physical state of the drug and increased surface area resulted in 80% LOV release within 10 min of an *in vitro* dissolution study in the simulated intestinal non-digestive medium (16). The hydrophilic silica surface which was rapidly wetted with release medium contributed to the prompt dissolution. A major concern with the immediate release porous silica carrier is however the generation of supersaturation followed by precipitation in the intestine.

More recently, a novel silica lipid hybrid (SLH) system has been developed which combines the advantages of LBDDS and porous silica carrier and has been demonstrated to improve the oral bioavailability of a number of poorly water-soluble drugs (17,18). The solid-state SLH formulation

was prepared from medium chain triglyceride and porous silica nanoparticles by firstly formation of mesoporous silica nanoparticles stabilized o/w emulsion and the subsequent spray or freeze-drying process. SLH formulations were free-flowing powders even with 80% liquid lipid content (19), and standard quality tablets could be prepared with the addition of mannitol in the formulation (20). The hybrid microparticles were composed of internal complex ordered matrices allowing higher drug loading and storage stability of more than a year. The three-dimensional internal porous nano-structure (pore size 20–100 nm) provided increased interfacial area and a solid support for controllable enzyme-mediated digestion of the encapsulated lipid (21) which results in significant improvement in the intestinal solubilization of several poorly soluble drugs such as celecoxib (18,19), indomethacin (17,22), and lovastatin (23). In particular, fine tuning of drug loading and dissolution of LOV was achieved depending on the size and geometry of different porous silica nanoparticles such as Aerosil 380 and Syloid 244FP. The synergistic effect of porous silica and self-emulsifying liquid lipid led to a two- to threefold improvement in the oral bioavailability compared to the pure LOV. However, as the mechanism suggests, the enzymatic digestion of the liquid lipid was prompt and the subsequent drug solubilization potentially generated a supersaturated aqueous environment and intestinal drug precipitation. There is a clear demand for a controlled delivery system for LOV which could be attained by applying solid lipids which are well-known for sustained lipid digestion. In addition, there has been increasing interest in solid lipid-based formulations to improve the oral bioavail-ability of LOV due to their potential to stimulate the intestinal absorption of the drug while avoiding hepatic metabolism (24–26).

The aim of the current study was to fabricate a novel porous silica-supported solid lipid carrier system to improve the solubilization of LOV through a controlled enzyme-mediated lipid digestion pathway. Our specific interest was to compare and contrast the roles of nanostructure and lipid loading level in releasing LOV from the silica-solid lipid matrix. Investigating the role of nanostructure in improving solid lipid digestion and *in vitro* drug release would provide further understanding of the mechanism of solubilization and of the behavior of LOV in the intestinal environment (27).

MATERIALS

Glyceryl monostearate, GMS (Geleol Mono and diglyc-erides NF), was kindly donated by Gattefosse (Sydney, Australia). Fumed hydrophilic silica nanoparticles (Aerosil® 380, A) and micronized synthetic amorphous silica micropar-ticles (Syloid 244FP, S) were supplied by Evonik Degussa (Essen, Germany) and Grace Davison Discovery Sciences (Rowville, Australia), respectively. LOV was sourced from Tecoland (CA, USA). For simulation of *in vitro* digestive conditions—sodium taurodeoxycholate (NaTDC), trizma ma-leate, type X-E L-α-lecithin (approximately 60% pure phos-phatidylcholine, from dried egg yolk), porcine pancreatin extract, calcium chloride dihydrate, and sodium hydroxide pellets were supplied by Sigma-Aldrich (Australia). For simulation of *in vitro* dissolution conditions, sodium di-hydrogen orthophosphate, di-sodium hydrogen *ortho*

phosphate, sodium dodecyl sulfate (SLS), and sodium hy-droxide pellets were purchased from Chem-Supply (Austra-lia). All other chemicals were of analytical grade and used as received. High purity MilliQ (MA, USA) water was used throughout the study.

METHODS

Drug-Free SSL

Preparation of SSL

Silica-supported solid lipid particles (SSL) were prepared using an immersion/solvent evaporation method (Fig. 1). Firstly, a known quantity of solid lipid (GMS) was dissolved in the solvent (dichloromethane, DCM). A known quantity of silica was then added to the lipid-solvent solution, and the resulting mixture was stirred using a magnetic stirrer. After 48 h, the bulk of the solvent was removed using a rotary evaporator (Rotovapor® R210, BÜCHI, Switzerland). Final-ly, the evaporated solids were placed in an oven at 40–50°C for an hour to remove residual solvent.

A series of SSL formulations were prepared using two types of silica (A and S) with differing physical properties (listed in Supplementary Table I) and lipid concentrations varying between 10% and 40%. A complete listing of the SSL formulations prepared is provided in Table I.

Physicochemical Properties

The SSL particles were analyzed for redispersed particle size using laser diffraction (Malvern Mastersizer 2000, Malvern, UK). Particle size data was collected at 5-min intervals for a period of 20 min after redispersing in water at a speed of 1000 rpm.

The surface morphology of the SSL-A and SSL-S was investigated using a scanning electron microscope (FEI Quanta 450 FEG ESEM, USA) at an accelerating voltage and working distance range of 10–30 kV and 0.5 μm–11.4 mm, respectively. Powdered samples were deposited onto double-sided adhesive carbon tape and sputter coated with carbon. Elemental spectra of the SSL particles were obtained from an energy-dispersive X-ray analysis (EDAX) using an EDAX Apollo X SDD EDX detector for localization and qualitative indication of each component within the hybrid material.

Lipid loading of the SSL particles was determined using thermal gravimetric analysis (TA Instruments, Sydney, Aus-tralia). Samples of approximately 10 mg were heated from 20 to 600°C at a rate of 10°C/min under a nitrogen gas purging. Associated TA Universal Analysis software was used to calculate the weight loss (after correction for the moisture and silica content) corresponding to the lipid content of the SSL samples.

In Vitro Lipid Digestion

Lipolysis studies were conducted using a TitraLab® 854 pH stat titration apparatus (Radiometer Analytical, Copen-hagen, Denmark) according to the method described by Sek *et al.* (28). SSL powder containing ~100 mg lipid was dispersed into 20 ml buffered micellar solution in a
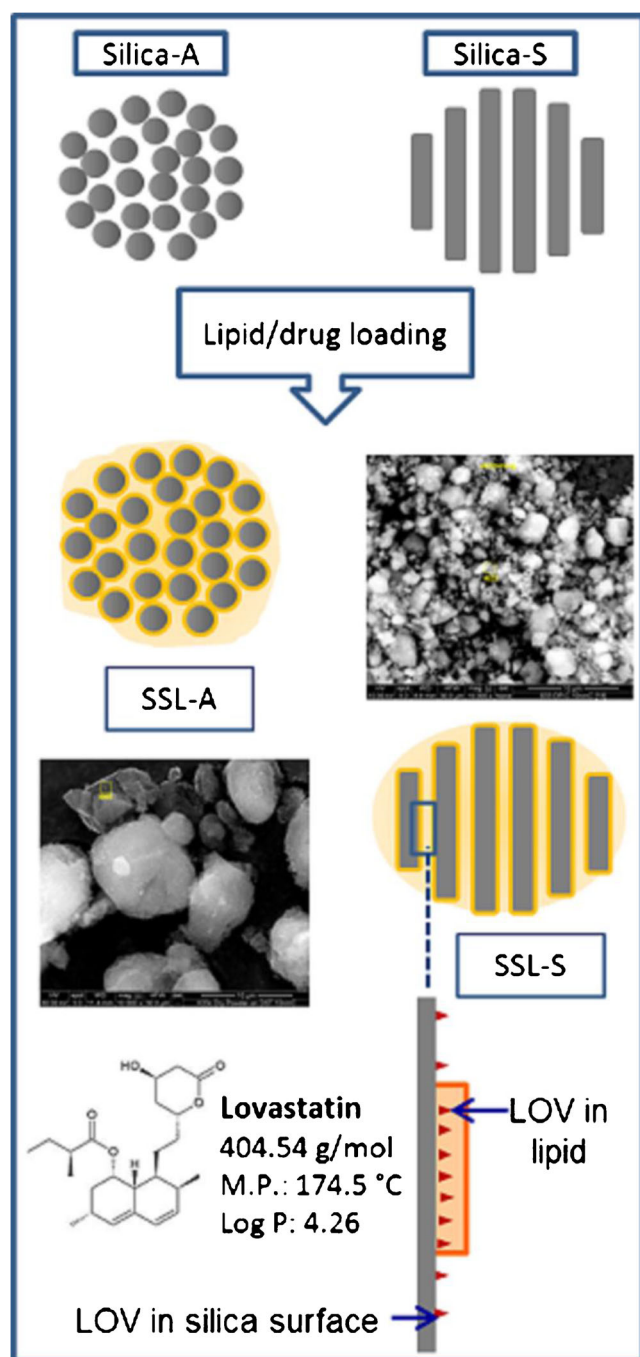
Fig. 1. Schematic showing the preparation of SSL particles. The solid lipid, GMS, is loaded into the porous network of silica (A and S) using a solvent evaporation method. The SEM images show larger and more compact aggregates of SSL-A when compared with the small aggregated clusters formed by SSL-S particles. LOV (model drug), together with GMS, was loaded into silica-S to produce LOV-SSL. The magnified *inset* demonstrates the possible LOV loading within the porous network of silica-S

thermostated glass reaction vessel maintained at a temperature of 37°C. Pancreatin extract (2 ml) was added into the digestion medium to initiate the lipolysis at a pancreatic activity rate of 1000 TBU/ml. NaOH (0.2 M) was then used to titrate the free fatty acids (FFA) generated in the digestion medium and to maintain the pH which was pre-set in the instrument beforehand. The "Titrameter 85" titration software was used to record the cumulative volume of NaOH used for the titration of the FFA generated in the reaction vessel at 5-s intervals. The data (determined in triplicate) was presented as a mean ± standard error of the mean (SEM).

A blank experiment was also conducted using this method to determine the amount of background fatty acids produced by components other than the studied lipid vehicles.

A pure GMS micellar dispersion (GMS MD) was used as a control for the lipolysis studies and was prepared by adding the melted lipid to the intestinal medium at 70°C and stirring at this temperature for 5 min. The particle size of the GMS MD was limited to the sub-micron range which was ensured by dynamic light scattering (Zetasizer Nano, Malvern, UK).
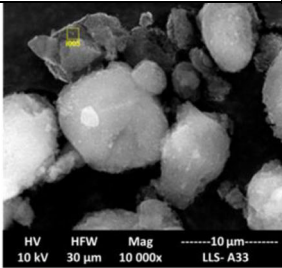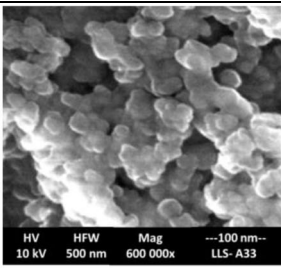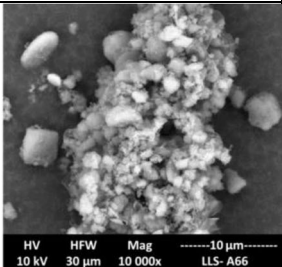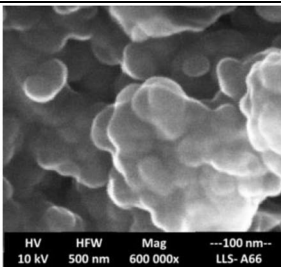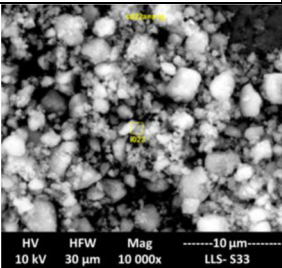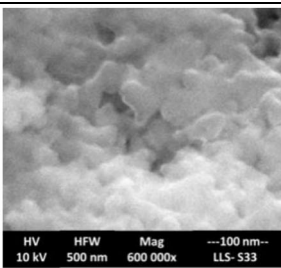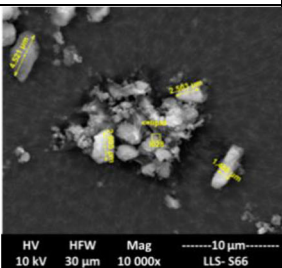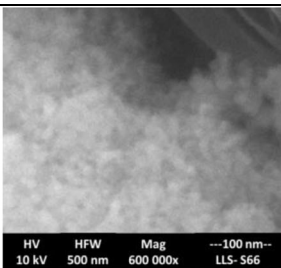
LOV-Loaded SSL

LOV Assay

LOV was assayed using a HPLC system (Shimadzu Corporation, Japan) consisting of a series of LC-20ADXR pumps, a SIL-20ACXR autosampler, a CTO-20AC column oven, and a SPD20A variable UV detector set at 238 nm. A Phenomenex RP-18 analytical column (5 µm, 4.6 mm ID × 250 mm) was used to conduct the chromatographic separation. The mobile phase was a mixture of acetonitrile and 10 mM phosphoric acid (13:7 *v/v*, pH 3.0), eluted at a flow rate of 1.5 ml/min. The limit of detection (LOD) and the limit of quantification (LOQ) were 5 and 15 ng/ml, respectively. A series of working solutions with concentrations ranging from 0.1 to 100 µg/ml (without the addition of an internal standard) were used for generating the linear calibration curve by plotting the chromatographic peak area *versus* LOV concentrations, *i.e.*, $y = 107161x - 995.54$ ($R^2 = 0.9999$). All analytes were diluted suitably to meet the calibration concentration range, and the samples were injected at a volume of 50 µL at ambient temperature.

Preparation, Drug Loading, and Molecular State of LOV-Loaded SSL

LOV-loaded SSL formulations were produced using silica-S only due to its superior solid lipid loading characteristics in comparison with silica-A. Three LOV-SSL formulations were prepared at lipid loading levels of 33%, 50%, and 66% (*w/w*) using the method described in the "Preparation of SSL" section. LOV was added to the solvent-lipid solution to its 100% equilibrium solubility in GMS (predetermined as 82 mg/g at 70°C) before the silica addition. LOV-loaded Syloid 244FP (LOV-S244) particles, a control for release studies, were prepared without the addition of GMS in the solvent mixture. Drug loading of these formulations was determined using a solvent extraction method. A sample of approximately 10 mg powder was mixed with 5 ml methanol (this provides an extraction efficiency of 100 ± 1%) to extract the encapsulated LOV. The mixture was centrifuged at 4500 rpm for 15 min and the supernatant analyzed to determine the LOV content using HPLC. The molecular states of the LOV-SSL33 (SSL-S with the highest studied drug

Table I. SSL Formulation Details Including Lipid/Silica Weight Ratios, Associated Lipid Content, and Redispersed Particle Size (D(0.9)) in Water (After 20 Min of Redispersion)

SSL	Lipid: silica ratio	Lipid load (%)	Redispersed size (μm)	SEM image		EDAX elemental analysis (%)		
				Low resolution image	High resolution image	C	O	Si
A 33	1:2	32.3 ± 0.4	57.5			28.9 ± 12.9	40.8 ± 8.5	34.3 ± 4.0
A 50	1:1	50.3 ± 1.5	-	-	-	-		
A 66	2:1	65.7 ± 6.1	482			52.1 ± 10.1	28.1 ± 10.9	19.8 ± 4.8
S 33	1:2	31.3 ± 0.2	20.3			33.9 ± 11.1	33 ± 8.7	32.5 ± 3.5
S 50	1:1	47.1 ± 1.6	-	-	-	-		
S 66	2:1	63.5 ± 1.7	90.4			56.3 ± 8.1	27.4 ± 9.3	14.9 ± 3.8

Scanning electron microscope images of SSL-A33, A66, S33, and S66 show the surface morphology of these formulations. The EDAX analysis provides a rough estimate of location and composition of individual components such as C, O, and Si

loading) and LOV-S244 were analyzed using differential scanning calorimeter (DSC, TA instruments, Australia). A LOV-silica physical mixture (prepared in the same ratio as in the LOV-SSL33) was used as the standard for this study. Each sample was heated in a sealed aluminum pan at a rate of 5°C/min over a temperature range of 25-200°C under N_2 gas flow (70 ml/min).

In Vitro Drug Dissolution

In vitro dissolution of unformulated LOV and the LOV-SSL formulations were investigated in both digesting and non-digesting conditions. Drug dissolution in non-digestive conditions was carried out under simulated intestinal sink and non-sink conditions using a USP 23 type II dissolution

apparatus (Vankel Industries Inc., USA) operated at 75 ± 0.02 rpm and 37°C. To investigate the drug release in simulated intestinal sink conditions, *i.e.*, the volume of medium at least three times that required to form a saturated solution of drug substance (29), SSL samples containing 2.5 mg LOV were added to the 900 ml of phosphate-buffered saline (PBS) containing 0.02% SLS (pH 7.4). Effect of non-sink conditions was evaluated by increasing the dose of LOV to 5 mg in the same dissolution medium. During the dissolution studies, 4-ml aliquots were drawn at fixed time points (up to 3 h) and replaced with fresh medium. Samples were immediately filtered (Millipore filter, 0.22 μm) and diluted with the HPLC mobile phase solution to meet the standard curve range. The diluted samples were then analyzed by HPLC to determine the drug content in the dissolution medium.

The solubilization level of LOV in the simulated intestinal medium under digestive conditions was also examined. Each formulation sample containing 3 mg LOV was added in a 20-ml fasted state release medium. During the 60-min release study, 1 ml aliquots were collected at each specified time interval. Each aliquot was dispensed into a centrifuge tube prefilled with 10 μl of 0.5 M 4-bromophenylboronic acid solution which acts as an enzyme inhibitor to stop the digestion process. Samples were centrifuged at 22,000 rpm for 1 h (37°C). The aqueous phase was separated and analyzed for LOV content using HPLC.

RESULTS AND DISCUSSION

Drug-free SSL

Preparation and Physicochemical Properties

Drug-free SSL-A and SSL-S were fabricated at lipid loading levels of 33%, 50%, and 66% (*w/w*) using the two types of silica (A and S) to produce SSL-A33 and SSL-S33, SSL-A50 and SSL-S50, and SSL-A66 and SSL-S66. A schematic for the preparation method is presented in Fig. 1. Visually, no difference was observed between the appearance of SSL-A and SSL-S. All of the SSL formulations prepared in this study were white agglomerated powders and higher solid lipid content (*e.g.*, 66%) increased the cohesiveness of the powders.

The impact of lipid-loading levels on the redispersed particle size and morphology of SSL was assessed. The particles sizes of SSL-A and SSL-S after 20 min of redispersion have been detailed in Table I. SSL-A33 retained the physical characteristics of silica-A (Supplementary Table I) and produced relatively larger (57.50 μm) agglomerated particles than SSL-S33s (20.31 μm). SSL-A66 and SSL-S66 produced larger redispersed particles than the lower lipid containing formulations, *i.e.*, 482 and 90 μm, respectively. Higher solid lipid content increased the adhesion of these particles, and re-aggregation of particles was observed for these two formulations after 15 min (data not shown). The measured redispersed sizes are therefore not of the individual particles but are rather the sizes of the aggregates containing cohesive particles of different sizes. SEM images of SSL-A33 and SSL-A66 show a porous and uniform network formed by the aggregation of primary nanoparticles (Table I). The

higher lipid loading of SSL-A66 resulted in significantly larger aggregated particles within this formulation than that of SSL-A33.

The morphology of both types of SSL was further analyzed by SEM using electron beams of different energies. Firstly, the low-energy secondary electron beam was passed through the samples, revealing that the surfaces of individual particles were round and smooth possibly due to the adsorbed lipid layer on the silica surface. Images obtained through the high energy backscattered electron beam detailed the inside of the aggregated particles showing the presence of denser objects—considered to be the silica (data not shown). Non-uniform distributions of silica-lipid hybrid were evident for both SSL formulations; however, SSL-S66 was shown to contain larger aggregates than SSL-S33. EDAX analysis confirmed the homogenous distribution of Si, C, and O throughout the particles in all four SSL formulations. Higher silica content and lower percent weight ratio of C *versus* Si were confirmed for both types of SSL-33s compared to SSL-66s.

The lipid content of SSL formulations was determined using thermogravimetric analysis (TGA) (Table I). Both SSL-A and SSL-S showed high lipid loading capacity which is attributed to the large surface area available for lipid adsorption (380 and 311 m^2/g for silica-A and S, respectively).

In Vitro Lipid Digestion

Solid lipid digestion from the SSL particles was assessed under a fasted state simulated intestinal condition. Figure 2 shows that the digestion profile of the solid lipid was enhanced 1.5- to 2-fold when loaded into the porous silica nanostructure. Of the lipid content, 42−53% was digested from the three SSL-S formulations over a period of an hour, whereas the corresponding amount was 26.2% for GMS MD. The considerably enhanced digestion was not only as a result of the significantly increased interfacial area, but hydrophilic silica provided solid support for lipase adsorption (30). This is consistent with the previous finding that the nanostructure of silica played an important role in controlling the digestion of liquid lipid (21). It should be noted that at the beginning of digestion, all the lipid substrate is accessible to the lipase enzyme. However, once the digestion has started, the inefficient removal of digestion products from the interface reduced the extent of lipase binding which in turn reduced the rate of further solid lipid digestion (21). In addition, there is a reduction in the surface area of lipid available for digestion which caused the reduced profile of lipolysis.

The lipid loading levels had a significant impact in controlling the lipolysis rate and extent of the three SSL-S formulations studied. The greatest extent of digestion was achieved from SSL-S33 and was two times higher than that observed with the digestion of GMS MD. The lower loading level in SSL-S33 is considered to have created a thin film of solid lipid within the silica pores which left sufficient exposed silica surfaces for lipase adsorption. It was previously demonstrated by Joyce *et al.* that the optimal loading of a long chain liquid lipid into silica-S to achieve a close packed monolayer coverage is approximately 29% (21). This type of coverage has been demonstrated to maximize the lipolysis profile due to the provision of increased surface area and
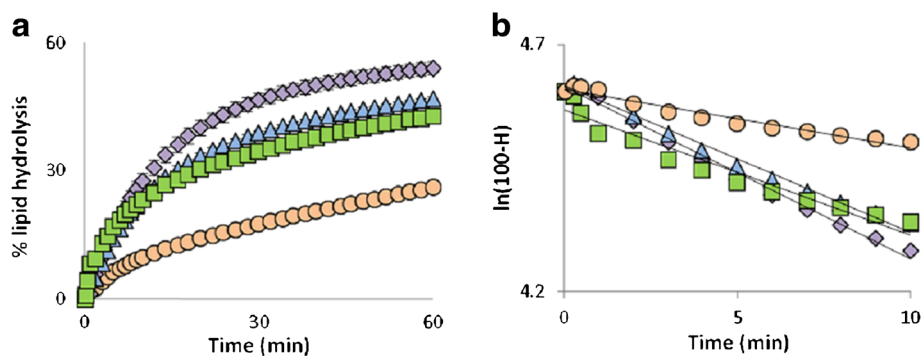
Fig. 2. a *In vitro* lipid digestion profile and **b** pseudo-first-order kinetics fit of GMS MD ⬡, SSL-S33 ◆, SSL-S50 ▲, and SSL-S66 ◼ under simulated fasted intestinal conditions at 37°C. ($n = 3$, mean ± SEM)

accessibility for lipase to the lipid-water interface (31). It is likely that the 31.28% solid lipid created an almost monolayer to sub-multilayer in SSL-S33, thereby increasing the opportunity for lipase enzyme to diffuse into the pore or adsorb to the surface. The lipolysis profile of SSL-S50 and SSL-S66 was similar, *i.e.*, lying in between those of SSL-S33 and the GMS MDs. Considering the findings of Joyce *et al.*, it is expected that the higher lipid loading level in SSL-S50 and SSL-S66 created a multilayer of solid lipid coverage and reduced levels of exposed silica surfaces hence limiting the lipase adsorption capability of these formulations. Moreover, the adsorption and insufficient removal of digestion products have been shown to create a barrier to further lipase binding to the lipid-silica interface (32)—it is expected that this contributed to the reduced digestion extent seen for SSL-S50 and SSL-S66 formulations. The lipolysis profile of the SSL-S formulations showed a good fit ($R^2 > 0.95$) to the pseudo-first-order kinetic model: $\% H = 100(1 - e^{-kt})$ where H is the lipolysis percentage, k is the pseudo-first-order release constant, and t is the time in minute. The lipolysis rate constants calculated for the initial 10 min of digestion have been listed in Supplementary Table II. It can be seen that the initial rate constant for all three SSL-S formulations is two- to threefold higher than that determined for the GMS MD. The trends in the lipolysis rate constants determined were SSL-S33 > SSL-S50 > SSL-S66 > GMS MD. The rate constant values of the three SSL-S formulations which have been analyzed using one-way analysis of variance (ANOVA) do not differ significantly around the mean rate constants ($p > 0.05$).

A similar analysis was performed for the three SSL-A formulations (Fig. 3) and, as per the SSL-Ss, the formulation which resulted in the highest lipid digestion rate and extent was that with the lowest lipid loading level (*i.e.*, SSL-A33). The other two followed similar lipolysis profiles in the same order of lipid loading. Interestingly, the lipolysis profiles of SSL-S were slightly higher than those of SSL-A at all three lipid loading levels tested. It is likely that the slightly larger and more organized pore distribution in silica-S allowed easier access for the lipase enzyme to adsorb onto the solid lipid interface in its active conformation (33). Furthermore, the higher redispersibility of SSL-S compared to that of SSL-As as indicated by the smaller redispersed particle sizes also contributed to the enhanced solid lipid interfacial area for lipase adsorption.

LOV-Loaded SSL

Physicochemical Characterization of LOV-SSL

The LOV-loaded SSL formulations were similar in appearance (*i.e.*, cohesive powders) to their drug-free counterparts. Ninety percent of the LOV-SSL particles were below 91.81 μm in diameter after being redispersed in water for 30 min (Table II). LOV-SSL 50 and LOV-SSL 66 particles were determined to be similar in size to their drug-free counterparts; however, the particle size of LOV-SSL 33 was determined to be three times larger than the drug-free SSL-S33 particles. This is probably due to the coalescence of excess silica nanoparticles.
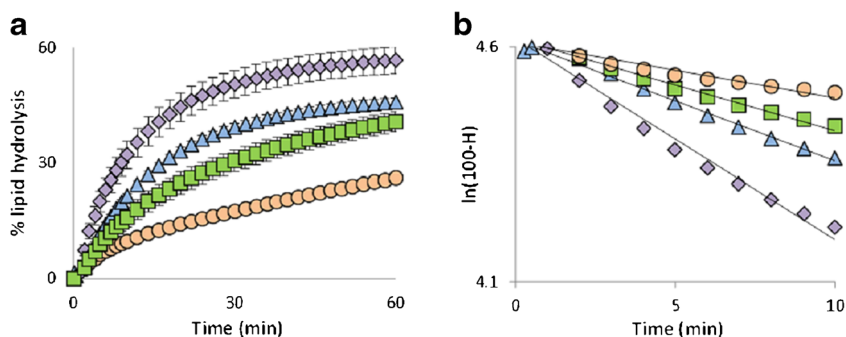

Fig. 3. a *In vitro* lipid digestion profile and **b** pseudo-first-order kinetics fit of GMS MD ⬡, SSL-A33 ◆, SSL-A50 ▲, and SSL-A66 ◼ under simulated fasted intestinal conditions at 37°C. ($n = 3$, mean ± SEM)

Table II. Physicochemical Properties of LOV-SSL Formulations

Formulation	Redispersed particle size in water (μm)	Lipid load (%) (*w/w*)	Drug load (%) (*w/w*)
LOV-SSL 33	70.88	34 ± 1.29	1.97 ± 0.06
LOV-SSL 50	87.87	50 ± 0.39	1.59 ± 0.19
LOV-SSL 66	91.81	65 ± 3.57	1.78 ± 0.06

LOV was loaded at 100% saturation level in the solid lipid which correlated to 1.59–1.97% (*w/w*) in the SSL formulations. A small endothermic peak was observed at 174.5°C in the DSC profiles of pure LOV and silica-S physical mixture indicating the presence of LOV in the crystalline state (Fig. 4). Absence of any crystalline peaks in the DSC profiles thus confirmed the non-crystalline or amorphous molecular state of the LOV within the SSL and LOV-S244 formulations.

In Vitro Drug Dissolution (Non-Digestive and Digestive Conditions)

Non-Digestive Condition In vitro dissolution studies were first performed in simulated intestinal non-digestive conditions (PBS containing 0.02% SLS, pH 7.2 at 37°C). The solubility of LOV in the release medium was determined to be 9.04 μg/ml; LOV was dosed at a level below solubility in all cases, *i.e.*, 5 mg equivalent LOV per 900 ml medium. The drug dissolution from LOV-S244 was rapid and straightforward attributing to the unrestricted availability of the drug within the medium (Fig. 5). Over 50% of the drug was released from LOV-S244 within 15 min; this performance is comparable to the previously reported LOV dissolution profiles obtained from a porous silica-based carrier system (16). The physical state of the raw drug was altered by spatially confining it within the nanoporous silica. The non-crystalline or amorphous state of the drug combined with the increased surface area provided by the porous silica played a vital role in the fast dissolution. Also, the large number of hydroxyl groups present on the surface of the mesoporous silica helped to reduce the contact angle with water which also resulted in the rapid drug release (34). However, the nanostructured solid lipid-loaded silica matrix also improved the *in vitro* solubilization of LOV compared to the LOV-lipid suspension and the unformulated drug which was three- to

Fig. 4. DSC thermograms of **a** LOV-S244, **b** physical mixture of LOV and silica-S, and **c** LOV-SSL33 formulation shown in *green*, *blue*, and *purple lines*, respectively

sixfold higher in the first hour of the study. All three samples demonstrated continuous LOV release over the 3 h of the dissolution period while a rapid reduction in drug release was observed for LOV-SSL33 after the first hour. The drug dissolution profile of LOV-SSL33 can be divided into three phases: the initial fast release phase (0–1 h), reduced release phase (1–2 h), and lastly a period of sustained release phase (2–3 h). It is noted here that a common solvent was used to prepare the LOV-SSL33 which gives no selectivity for LOV towards lipid or silica. It is therefore possible that some of the drug had been directly adsorbed onto the silica surfaces (see schematic in Fig. 1): this would have allowed them to be more accessible and dissolve more rapidly in the medium at the beginning of the release study which could explain why over 60% of the drug was released during this period (35). Moreover, the SEM images suggest that the SSL particles are composed of various sized pores. There is the possibility that in the first hour of dissolution drug is released from the larger pores which are reasonably well accessible to the medium. The initial burst release may cause a local precipitation of drug (36) and due to the higher affinity of the drug towards lipid compared to the release medium would re-adhere to the SSL particles (37). Plausibly, this re-adhesion of the drug and associated release of end products (*e.g.*, silica, lipid and SLS mixed species) caused blocking of the small pores and reduced the effective surface area for dissolution. These factors would in turn reduce the solubilizing capacity of the particles which could be the cause for the rapid reduction seen in the dissolution during the second hour of the study. Finally, a percentage of the drug is likely to exist in a soluble form in the long chain solid lipid and strongly adsorbed in the silica pores. Consequently, the drug would be released in a sustained manner from the pore channel (38)—this is a plausible explanation for the sustained drug release observed in the third hour of the experiment.

The lipid loading level in the porous silica showed significant impact in the drug release profiles of the three SSL-S formulations (Fig. 6). In the simulated intestinal sink conditions (2.5 mg equivalent LOV per 900 ml PBS containing 0.02% SLS, pH 7.2 at 37°C), LOV-S244, the sample containing no lipid, demonstrated the maximum drug release extent. With an initial burst release phase taking place within the first 30 min, LOV-S244 was determined to release 50% of the drug within 3 h. The aqueous medium was absorbed into the mesoporous silica and the unrestricted availability of the drug within the medium caused rapid dissolution/diffusion of the drug from silica pores. Introducing solid lipid into the porous silica was found to result in a reduced extent of initial drug release. All three LOV-SSL formulations demonstrated
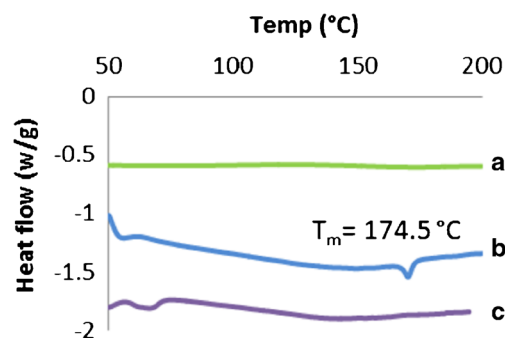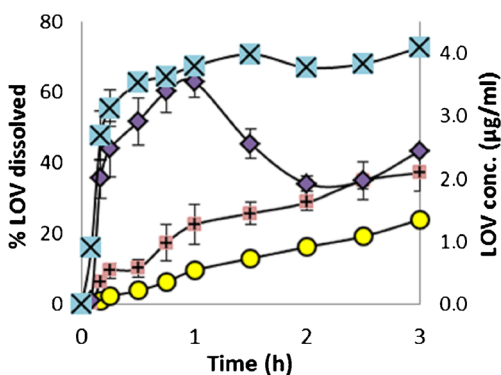
Fig. 5. *In vitro* release of LOV from LOV-S244 [×] compared to LOV-SSL33 [♦], LOV-lipid suspension [+], and unformulated LOV [○] in simulated intestinal non-sink condition (PBS containing 0.02% SLS, pH 7.2, 37°C, concentration 5.5 µg/ml). ($n = 3$, mean ± SEM)

an initial fast release phase within 30 min of the release experiment commencing and a reduced rate until the 2 h time point. It is possible that the solid lipid layers inside the porous silica caused a reduction in the available interfacial area and contact angle for efficient wetting by the dissolution medium, thus reducing the drug dissolution. The LOV-SSL 33 which contains the lowest lipid loading level of the formulations tested revealed a higher drug release profile (36% release over 3 h) compared with the other two formulations—LOV-SSL 50 (21.6%) and LOV-SSL 66 (14.2%). The higher lipid loading in LOV-SSL 66 causes more compact nanostructure and blocking of pores compared to the lower lipid-loaded samples and jeopardizes the drug accessibility by the dissolution medium. It is expected that beyond this lipid loading level, the reduced available surface area and reduced nanostructure decrease the ability of the drug to diffuse out resulting poor drug solubilization. A similar study was performed by Larsen *et al.* (2013) for SNEDDS formulations loaded with cinnarizine at different saturation solubility, and no significant difference in oral bioavailability was noticed with the same drug dose administration, which disregards the role of lipid vehicle amount in the formulation (39). Another study performed by the same research group showed that inorganic porous carriers (magnesium aluminometasilicate) restrict the drug
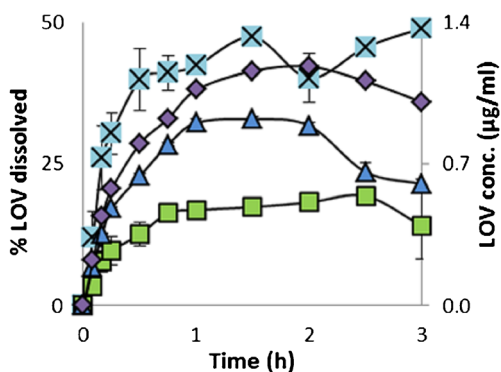
solubilization from a SNEDDS formulation in the intestinal digestive condition (40). Given that S244 has three to four times larger pores compared to the former inorganic material (41,42), the loaded drug could easily diffuse out to the release medium and the drug dissolution was improved (14). The nanostructure produced by solid lipid loading in porous silica therefore has a major impact on the morphology of SSL formulations and thus provides fine control over the drug dissolution process.

Digestive Condition The dynamic drug solubilization from the LOV-lipid suspension, LOV-S244 and LOV-SSL 33 formulations were tested in a simulated intestinal digestive condition (Fig. 7). Pancreatic lipase was added to simulate the lipase in the *in vivo* condition. A time-dependent gradual increase in the aqueous phase concentration of LOV was noticed when the drug was dosed as a lipid suspension, and a final concentration of 16.7 µg/ml was attained at 120 min which was the lowest among the three samples tested. The bulk lipid suspension possessed lower interfacial area for lipase adsorption in comparison to the nanostructured formulations LOV-S244 and LOV-SSL 33. Although the drug was loaded as a molecular dispersion, the poor digestibility of the solid lipid could not support generating an adequate amount of digestion end product to retain the drug in the release medium. The aqueous phase concentration achieved from the LOV-S244 dissolution study was 22.2 µg/ml which is 1.3-fold higher than that achieved by the LOV-lipid suspension. It is expected that the improved LOV solubilization from this formulation was assisted by the increased surface area provided by the porous silica-S platform. Moreover, the hydroxyl group-rich silica surface reduces the contact angle with the release medium and assists in prompt wetting which permitted improved drug dissolution (34). The amorphous state of LOV also contributed towards the higher solubility of the drug in the aqueous medium. The highest aqueous phase LOV concentration (58.9 µg/ml at 120 min) was achieved in the case of LOV-SSL 33 which was 2.7 to 3.5 times superior to that of the LOV-S244 and LOV-lipid suspensions. A possible explanation for this is that the porous nanostructure of the LOV-SSL 33 offered an increased proportion of an oil–water interface (Fig. 8)
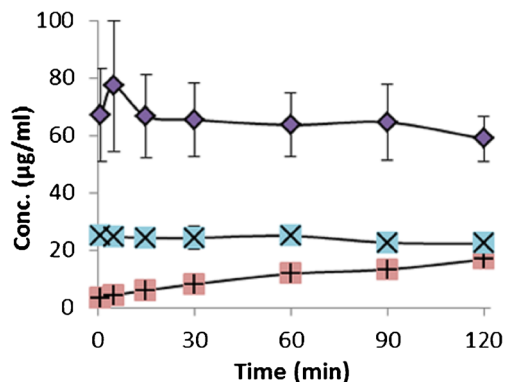

Fig. 6. *In vitro* drug release from the LOV-S244 [×], LOV-SSL33 [♦], LOV-SSL50 [▲], and LOV-SSL66 [■] in simulated intestinal sink condition (PBS containing 0.02% SLS, pH 7.2, 37°C, concentration 2.8 µg/ml). ($n = 3$, mean ± SEM)

Fig. 7. *In vitro* drug solubilization from LOV-lipid suspension ([+]), LOV-S244 [×], and LOV-SSL 33 [♦] during lipolysis studies in simulated intestinal digesting conditions (fasted stated mixed micellar buffered solution, pH 7.4, 3°C, maximum concentration 150 µg/ml). ($n = 3$, mean ± SEM)
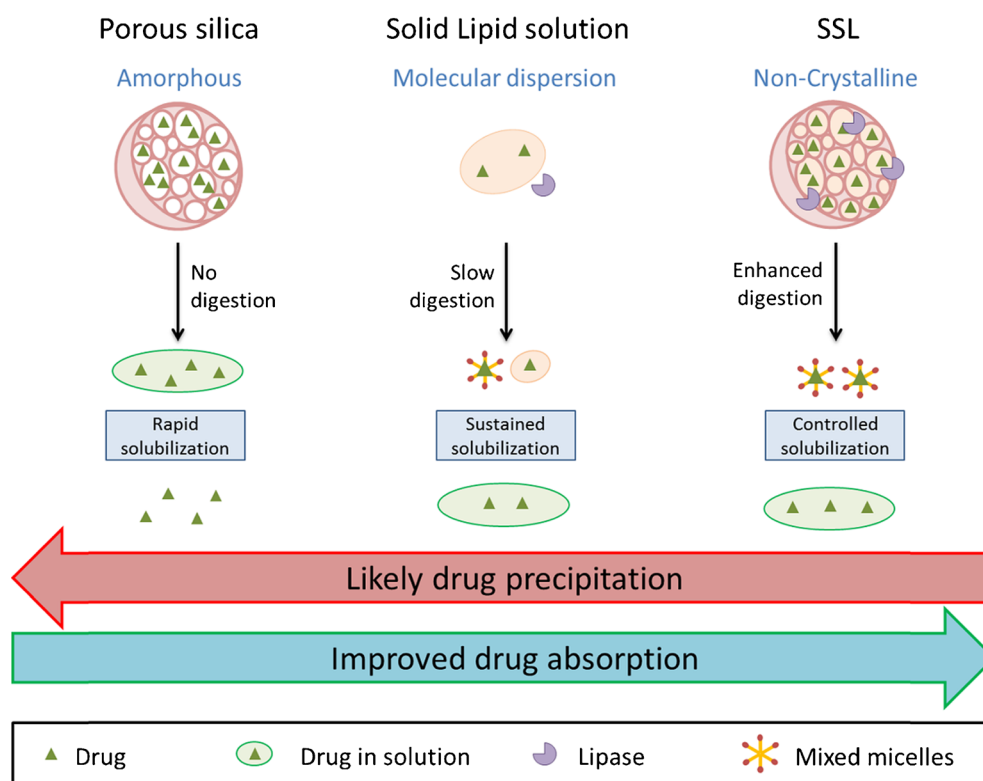
Fig. 8. Proposed mechanism of controlled solubilization from the porous silica-supported solid lipid (SSL) particles in the simulated intestinal digestive condition. The hydrophilic porous silica-supported nanostructure facilitates lipase adsorption and enhances the solid lipid digestion. The mixed micelles generated during the digestion result in controlled drug solubilization

and the surface chemistry of hydrophilic silica maximized the potential for lipase adsorption onto the silica surface allowing enhanced digestion of the entrapped solid lipid. The lipolysis end products and colloidal mixed micelles generated during the solid lipid digestion supported further solubilization of the non-crystalline LOV encapsulated in the silica-supported solid lipid particles. This result is consistent with the one obtained from a parallel study by our group (23) and provides a strong indication of the synergistic role of lipid and nanoporous silica in improving the solubilization of LOV.

CONCLUSION

The loading of solid lipid into nanostructured silica particles improve the digestibility of the lipid. The rate and extent of solid lipid digestion was controlled by altering the lipid content and the morphology within the nanostructure. LOV solubilization was noticeably improved when incorporated into a solid lipid-loaded silica nanostructure in comparison with their individual components under intestinal digestive conditions. This suggests that the synergistic role of nanostructured silica particles and solid lipid optimized the solubilization of LOV. The silica-supported solid lipid system has therefore been established as a more effective platform for LOV solid dosage formulations than the existing ones. In this way,

the novel formulation studied demonstrates potential for improving the solubilization of poorly soluble drugs.

REFERENCES

1. Amidon G, Lennernäs H, Shah V, Crison J. A theoretical basis for a biopharmaceutic drug classification: the correlation of in vitro drug product dissolution and in vivo bioavailability. Pharm Res. 1995;12(3):413–20.
2. Porter CJH, Trevaskis NL, Charman WN. Lipids and lipid-based formulations: optimizing the oral delivery of lipophilic drugs. Nat Rev Drug Discov. 2007;6(3):231–48.
3. Porter CJH, Pouton CW, Cuine JF, Charman WN. Enhancing intestinal drug solubilisation using lipid-based delivery systems. Adv Drug Deliv Rev. 2008;60(6):673–91.
4. Trevaskis NL, Charman WN, Porter CJH. Lipid-based delivery systems and intestinal lymphatic drug transport: a mechanistic update. Adv Drug Deliv Rev. 2008;60(6):702–16.

5. Zhu Y, D'Agostino J, Zhang Q-Y. Role of intestinal cytochrome P450 (P450) in modulating the bioavailability of oral lovastatin: insights from studies on the intestinal epithelium-specific P450 reductase knockout mouse. Drug Metab Dispos. 2011;39(6):939–43.

6. Chen CC, Tsai TH, Huang ZR, Fang JY. Effects of lipophilic emulsifiers on the oral administration of lovastatin from nanostructured lipid carriers: physicochemical characterization and pharmacokinetics. Eur J Pharm Biopharm. 2010;74(3):474–82.

7. Ge Z, Zhang X-x, Gan L, Gan Y. Redispersible, dry emulsion of lovastatin protects against intestinal metabolism and improves bioavailability. Acta Pharmacol Sin. 2008;29(8):990–7.

8. Mandal S. Microemulsion drug delivery system: design and development for oral bioavailability enhancement of lovastatin. SA Pharm J. 2011;78(3):44–50.

9. Yanamandra S, Venkatesan N, Kadajji VG, Wang Z, Issar M, Betageri GV. Proliposomes as a drug delivery system to decrease the hepatic first-pass metabolism: case study using a model drug. Eur J Pharm Sci. 2014;64:26–36.

10. Goyal U, Arora R, Aggarwal G. Formulation design and evaluation of a self-microemulsifying drug delivery system of lovastatin. Acta Pharma. 2012;62(3):357–70.

11. Suresh G, Manjunath K, Venkateswarlu V, Satyanarayana V. Preparation, characterization, and in vitro and in vivo evaluation of lovastatin solid lipid nanoparticles. AAPS Pharm Sci Technol. 2007;8(1):E162–70.

12. Seenivasan A, Panda T, Théodore T. Lovastatin nanoparticle synthesis and characterization for better drug delivery. Open Biotechnol J. 2011;5(1):28–32.

13. Tiwari R, Pathak K. Nanostructured lipid carrier versus solid lipid nanoparticles of simvastatin: comparative analysis of characteristics, pharmacokinetics and tissue uptake. Int J Pharm. 2011;415(1–2):232–43.

14. Xu W, Riikonen J, Lehto V-P. Mesoporous systems for poorly soluble drugs. Int J Pharm. 2013;453(1):181–97.

15. Vallet-Regí M, Balas F, Arcos D. Mesoporous materials for drug delivery. Angew Chem Int Ed. 2007;46(40):7548–58.

16. Wu C, Wang J, Hu Y, Zhi Z, Jiang T, Zhang J, et al. Development of a novel starch-derived porous silica monolith for enhancing the dissolution rate of poorly water soluble drug. Mater Sci Eng C. 2012;32(2):201–6.

17. Simovic S, Heard P, Hui H, Song Y, Peddie F, Davey AK, et al. Dry hybrid lipid–silica microcapsules engineered from submicron lipid droplets and nanoparticles as a novel delivery system for poorly soluble drugs. Mol Pharm. 2009;6(3):861–72.

18. Tan A, Simovic S, Davey AK, Rades T, Prestidge CA. Silica-lipid hybrid (SLH) microcapsules: a novel oral delivery system for poorly soluble drugs. J Control Release. 2009;134(1):62–70.

19. Yasmin R, Tan A, Bremmell KE, Prestidge CA. Lyophilized silica lipid hybrid (SLH) carriers for poorly water-soluble drugs: physicochemical and in vitro pharmaceutical investigations. J Pharm Sci. 2014;103(9):2950–9.

20. Bremmell KE, Tan A, Martin A, Prestidge CA. Tableting lipid-based formulations for oral drug delivery: a case study with silica nanoparticle–lipid–mannitol hybrid microparticles. J Pharm Sci. 2013;102(2):684–93.

21. Joyce P, Tan A, Whitby CP, Prestidge CA. The role of porous nanostructure in controlling lipase-mediated digestion of lipid loaded into silica particles. Langmuir. 2014;30(10):2779–88.

22. Simovic S, Hui H, Song Y, Davey AK, Rades T, Prestidge CA. An oral delivery system for indomethacin engineered from cationic lipid emulsions and silica nanoparticles. J Control Release. 2010;143(3):367–73.

23. Rao S, Tan A, Boyd BJ, Prestidge CA. Synergistic role of self-emulsifying lipids and nanostructured porous silica particles in optimizing the oral delivery of lovastatin. Nanomedicine. 2014;1–15.

24. Porter CJH, Charman WN. Uptake of drugs into the intestinal lymphatics after oral administration. Adv Drug Deliv Rev. 1997;25(1):71–89.

25. Venishetty VK, Chede R, Komuravelli R, Adepu L, Sistla R, Diwan PV. Design and evaluation of polymer coated carvedilol loaded solid lipid nanoparticles to improve the oral bioavailability: a novel strategy to avoid intraduodenal administration. Colloids Surf B: Biointerfaces. 2012;95:1–9.

26. Müller RH, Shegokar R, Keck CM. 20 years of lipid nanoparticles (SLN & NLC): present state of development & industrial applications. Curr Drug Discov Technol. 2011;8(3):207–27.

27. Porter CJH, Kaukonen AM, Taillardat-Bertschinger A, Boyd BJ, O'Connor JM, Edwards GA, et al. Use of in vitro lipid digestion data to explain the in vivo performance of triglyceride-based oral lipid formulations of poorly water-soluble drugs: studies with halofantrine. J Pharm Sci. 2004;93(5):1110–21.

28. Sek L, Porter CJH, Kaukonen AM, Charman WN. Evaluation of the in-vitro digestion profiles of long and medium chain glycerides and the phase behaviour of their lipolytic products. J Pharm Pharmacol. 2002;54(1):29–41.

29. The Dissolution Procedure: Development and Validation [database on the Internet]. 2013 [cited 22 Nov. 2013]. Available from: http://www.usp.org/usp-nf/notices/general-chapter-dissolution-procedure-development-and-validation.

30. Reis P, Holmberg K, Watzke H, Leser ME, Miller R. Lipases at interfaces: a review. Adv Colloid Interf Sci. 2009;147–148:237–50.

31. Wickham M, Garrood M, Leney J, Wilson PDG, Fillery-Travis A. Modification of a phospholipid stabilized emulsion interface by bile salt: effect on pancreatic lipase activity. J Lipid Res. 1998;39(3):623–32.

32. Li Y, Hu M, McClements DJ. Factors affecting lipase digestibility of emulsified lipids using an in vitro digestion model: proposal for a standardised pH-stat method. Food Chem. 2011;126(2):498–505.

33. Hanefeld U, Gardossi L, Magner E. Understanding enzyme immobilisation. Chem Soc Rev. 2009;38(2):453–68.

34. Jiang T, Wu C, Gao Y, Zhu W, Wan L, Wang Z, et al. Preparation of novel porous starch microsphere foam for loading and release of poorly water soluble drug. Drug Dev Ind Pharm. 2014;40(2):252–9.

35. Vallet-Regi M, Doadrio JC, Doadrio AL, Izquierdo-Barba I, Pérez-Pariente J. Hexagonal ordered mesoporous material as a matrix for the controlled release of amoxicillin. Solid State Ionics. 2004;172(1–4):435–9.

36. Aerts CA, Verraedt E, Depla A, Follens L, Froyen L, Van Humbeeck J, et al. Potential of amorphous microporous silica for ibuprofen controlled release. Int J Pharm. 2010;397(1–2):84–91.

37. Siegel RA, Rathbone MJ, editors. Overview of controlled release mechanisms. Fundamentals and applications of controlled release drug delivery. United States: Springer; 2012. p. 19–46.

38. Santamaría E, Maestro A, Porras M, Gutiérrez JM, González C. Controlled release of ibuprofen by meso-macroporous silica. J Solid State Chem. 2014;210:242–50.

39. Larsen AT, Åkesson P, Juréus A, Saaby L, Abu-Rmaileh R, Abrahamsson B, et al. Bioavailability of cinnarizine in dogs: effect of SNEDDS loading level and correlation with cinnarizine solubilization during in vitro lipolysis. Pharm Res. 2013;30(12):3101–13.

40. Christophersen PC, Christiansen ML, Holm R, Kristensen J, Jacobsen J, Abrahamsson B, et al. Fed and fasted state gastrointestinal in vitro lipolysis: in vitro in vivo relations of a conventional tablet, a SNEDDS and a solidified SNEDDS. Eur J Pharm Sci. 2014;57:232–9.

41. Tan A, Rao S, Prestidge CA. Transforming lipid-based oral drug delivery systems into solid dosage forms: an overview of solid carriers, physicochemical properties, and biopharmaceutical performance. Pharm Res 2013;1–25

42. Neusilin. Fuji Chemical Industries. Available from: http://www.neusilin.com/product/general_properties.php.